Effects of subfilter velocity modelling on dispersed phase in LES of heated channel flow

Journal of Physics: Conference Series **333** (2011) 012014 doi:10.1088/1742-6596/333/1/012014

Effects of subfilter velocity modelling on dispersed phase in LES of heated channel flow

Jacek Pozorski, Maria Knorps, Mirosław Łuniewski

Institute of Fluid-Flow Machinery, Polish Academy of Sciences,
Fiszera 14, 80952 Gdańsk, Poland

E-mail: {jp, mknorps, mirmir}@imp.gda.pl

Abstract. A non-isothermal turbulent flow with the dispersed phase is modelled using the Large Eddy Simulation (LES) approach for fluid, one-way coupled with the equations of point-particle evolution. The channel is heated at both walls and isoflux boundary conditions are applied for fluid. Particle velocity and thermal statistics are computed. Of particular interest are the r.m.s. profiles and the probability density function of particle temperature in the near-wall region. We compare our findings with available reference data for particle-laden, heated channel flow. Moreover, an open issue in LES is the influence of non-resolved (residual) scales of fluid velocity and temperature fields on particles. In the present contribution, we apply a stochastic model for subfilter fluid velocity at the particle positions that aims at reconstructing the effects of the smallest scales of turbulence on particle dynamics. We analyse the impact of this model on particle thermal statistics.

1. Introduction

Channel flows are important benchmarks because of the modelling issues representative of inhomogeneous and wall-bounded turbulence. For model validation, comprehensive data sets are available from the Direct Numerical Simulations (DNS). Despite their simple geometry, turbulent channel flows exhibit complex physical features, including the near-wall vortical structures that affect the temperature field. The presence of particulate phase only increases this complexity [1]. From the practical point of view, exact predictions of particle dynamics in the near-wall region, their separation on the walls, and temperature distribution in non-isothermal cases are desirable.

We consider the issue of particle motion one-way coupled with the non-isothermal fluid flow that is determined from the Large Eddy Simulation (LES). The temperature is assumed to be a passive scalar, so it does not affect the fluid motion. We analyse here the effect of subfilter fluid velocity field on the dispersed phase, called the subfilter particle dispersion. To this aim, a stochastic model of the Langevin equation type is applied for the residual fluid velocity along particle trajectories. First, we report results from a regular LES (with no reconstruction of the residual velocity) of particle-laden channel flow. The LES corresponds to the computational conditions of the DNS reference data: for the flow case defined by the COST Action benchmark [2], for the heated flow [3], and for the particle thermal correlations [4]. Following our earlier work on particle velocity statistics [5], we analyse the impact of the subfilter particle dispersion model on particle temperature statistics. We discuss these issues and present results obtained for the particle-laden, turbulent channel flow with isoflux conditions at the walls.

2. Governing equations for fluid and dispersed phase

The fluid phase is governed by the filtered Navier-Stokes equations. In the momentum equation for the large-scale velocity field $\bar{\mathbf{U}}_f(\mathbf{x},t)$, the resulting subgrid-scale (SGS) stress tensor is modelled through the subfilter viscosity ν_t, closed here with the dynamic (Germano-Lilly) approach [6]. The passive scalar equation for the filtered temperature $\bar{T}_f(\mathbf{x},t)$ takes the form

$$\frac{\partial \bar{T}_f}{\partial t} + \bar{U}_{f,i}\frac{\partial \bar{T}_f}{\partial x_i} = \frac{\partial}{\partial x_i}\left[\left(\frac{\nu_f}{\mathrm{Pr}} + \frac{\nu_t}{\mathrm{Pr}_t}\right)\frac{\partial \bar{T}_f}{\partial x_i}\right] \tag{1}$$

and the SGS heat flux term is closed with the subfilter thermal diffusivity ν_t/Pr_t (cf. Table 1).

Particles in the flow are assumed to be smaller than the Kolmogorov length scale and are treated here as point-particles. The mass and volume load of the dispersed phase are taken much smaller than 1, therefore the one-way momentum and energy coupling with the fluid phase is sufficient. We note that some recent computational studies address the motion and heat transfer of finite-size particles with two-way coupling between the phases, cf. [7] and references therein.

Simplified equations of motion for particles are applied here. Only the drag force term is considered, which is acceptable for heavy particles, $\rho_p \gg \rho_f$. The collisions of particles with the walls are assumed elastic (the particle wall deposition case was studied in [5]). The equations of particle motion and temperature evolution are:

$$\frac{d\mathbf{x}_p}{dt} = \mathbf{U}_p\,, \qquad \frac{d\mathbf{U}_p}{dt} = f_D\frac{\mathbf{U}^* - \mathbf{U}_p}{\tau_p}\,, \qquad \frac{dT_p}{dt} = f_\theta\frac{T^* - T_p}{\tau_\theta}\,. \tag{2}$$

The fluid velocity $\mathbf{U}^*$ and temperature T^* along the particle trajectory are obtained from the second order interpolation of the LES field. The particle momentum relaxation time $\tau_p = \rho_p d_p^2/18\rho_f\nu_f$ and thermal relaxation time $\tau_\theta = \rho_p c_p d_p^2/12\lambda_f$ are assumed to be equal in the present study. The Stokes number (the particle inertia parameter) is conveniently defined in wall-bounded flows as $St = \tau_p^+$ (viscous scaling). The coefficients f_D and f_θ are well-known, semi-empirical correction factors for the drag force and heat transfer, respectively [8].

Lower-inertia particles are more responsive to small-scale eddy structures and, since the fluid velocity field is deprived of subfilter (higher) frequencies, an additional subgrid model for fluid velocity seen by particles is needed. Let us decompose it as $\mathbf{U}^* = \bar{\mathbf{U}}^* + \mathbf{u}^*$, where $\bar{\mathbf{U}}^* = \bar{\mathbf{U}}_f(\mathbf{x}_p,t)$ is the part resolved in LES and $\mathbf{u}^*$ is the SGS contribution. As proposed in [9], we use a stochastic Langevin equation, aiming to mimic the evolution of fluid velocity at particle's position. This is done by adding a random term, representing the effect of fluctuations in the SGS fluid velocity on the dispersed phase. The subfilter particle dispersion model states:

$$du_i^* = -\frac{u_i^*}{\tau_L^*}dt + \sqrt{\frac{2\sigma_{\mathrm{sg}}^2}{\tau_L^*}}dW_i, \tag{3}$$

where dW_i is an increment of the Wiener process. The subfilter velocity scale $\sigma_{\mathrm{sg}} = (\frac{2}{3}k_{\mathrm{sg}})^{1/2}$ is obtained from the estimated kinetic energy lost by filtration (e.g., the Yoshizawa assumption with the dynamic procedure [10]), and $\tau_L^* = C_{sg}\bar{\Delta}/\sigma_{\mathrm{sg}}$ is the subfilter time scale of turbulence, where $\bar{\Delta}$ is the filter width and C_{sg} is the model constant responsible for the time correlation of the subfilter velocity and, consequently, for the amount of kinetic energy added to particles [9]. A separate model for subfilter temperature at the particle position has not yet been included.

3. Numerical solution

A fully-developed turbulent channel flow is computed at the Reynolds number, based on the friction velocity, of $Re_\tau = 150$ (a benchmark test case of the COST Action LES-AID, [2]).

Table 1. Simulation parameters

Symbol	Value	Description
Re_τ	150	Reynolds number based on friction velocity
Pr	0.7	Prandtl number (air)
Pr_τ	0.98	turbulent Prandtl number
C_{sg}	0.01, 0.05	SGS Langevin model constant
St	1, 5, 25, 125	particle Stokes number τ_p^+

More numerical simulation parameters are presented in Table 1. The pressure-driven flow was assumed periodic in the streamwise and spanwise directions. The size of the flow domain in the streamwise (x), wall-normal (y) and spanwise (z) directions was $4\pi h \times 2h \times (4/3)\pi h$, discretised with $64 \times 84 \times 64$ FV meshes. For the fluid LES, we used a finite volume, academic solver of second-order accuracy (`FASTEST3D` code – courtesy of Prof. M. Schäfer, TU Darmstadt, Germany). The mesh size Δy^+ (in wall units) varied from 0.17 at the wall up to 10 at the centerline. In the periodic directions, the mesh was uniform with $\Delta x^+ = 29.5$ and $\Delta z^+ = 9.8$. At the walls, the isoflux b.c. were imposed. The present case complements therefore that of [8] where the heated-cooled channel with isothermal b.c. was studied.

Computations were performed with the time step $\Delta t^+ = 0.097$. The dispersed phase was added to the flow once the statistically-steady fluid thermal state was achieved ($t^+ \approx 60\,000$). The total simulation time for the particle-laden channel flow with $C_{sg} = 0.01$ was $t^+ \approx 34\,000$, and with $C_{sg} = 0.05$ it was about 10 000. The presence of the stochastic model for the particles affected the convergence time of the computations. The large particles ($St = 125$) achieved a stationary near-wall concentration faster with the SGS dispersion model (after $t^+ \approx 17\,000$). The small particles ($St = 1$) without the model were rapidly converged (after $t^+ \approx 1000$), while in the presence of the model the concentration slightly varied even at $t^+ \approx 30\,000$.

4. Results

First, the LES fluid solution of the channel flow case was compared to the DNS data of Kasagi et al. [11]. Figures 1 and 2 show the mean and r.m.s. profiles of fluid temperature, respectively. The mean temperature obtained in the LES does not differ from the DNS one. However, the r.m.s. fluctuations in LES, although smaller in the central part of the channel, are higher near the walls and the peak r.m.s. value is somewhat shifted closer to the wall. Such a behaviour may be due to the LES effect on small structures.

In order to estimate the impact of the Langevin equation-based model on the dispersed phase statistics, we compare the r.m.s. velocity fluctuations for of $St = 1$ particles (Fig. 3) to available DNS data [2]. Three cases of LES are shown: without the SGS particle dispersion model (denoted by 'LES'), with the SGS stochastic model and constant $C_{sg} = 0.01$, and with the model and constant $C_{sg} = 0.05$. Even without an additional model for particles, the LES gives good results for the streamwise velocity fluctuations, where the absolute error is small. For the wall-normal and spanwise directions (not shown, but qualitatively similar), the velocity fluctuations are underestimated as compared to the DNS. The presence of the model, with $C_{sg} = 0.01$, does not cover for energy of small scales, unresolved in LES. Another model constant tested was $C_{sg} = 0.05$ and the velocity fluctuation profiles are more consistent with DNS in the near-wall region, but according to [5] the higher the value of C_{sg}, the larger the overestimation of particle wall deposition velocity. Consequently, as the model is too dispersive in terms of preferential concentration patterns (high values of C_{sg}), despite the correct amount of energy added to the flow, the particle concentration is at odds with the physical situation.

The r.m.s. fluctuations of particle temperature for $St = 1$ and 25 are shown in Figs. 4 and 6.

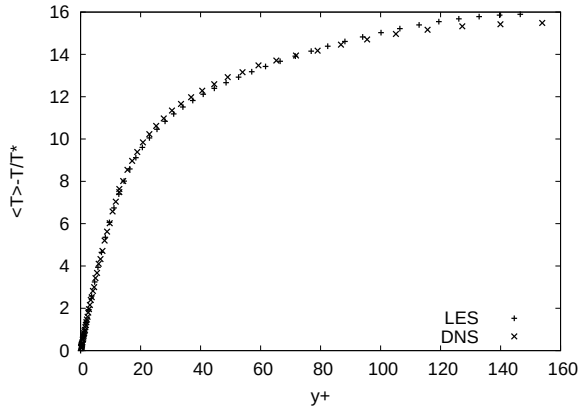

Figure 1. The mean fluid temperature: LES (+) and DNS (×) ref. data [11]

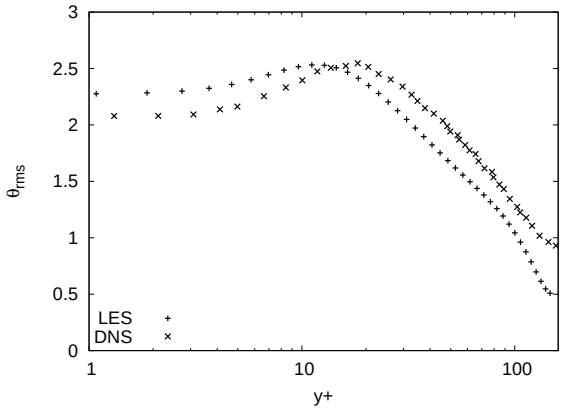

Figure 2. The r.m.s. fluid temperature: LES (+) and DNS (×) ref. data [11]

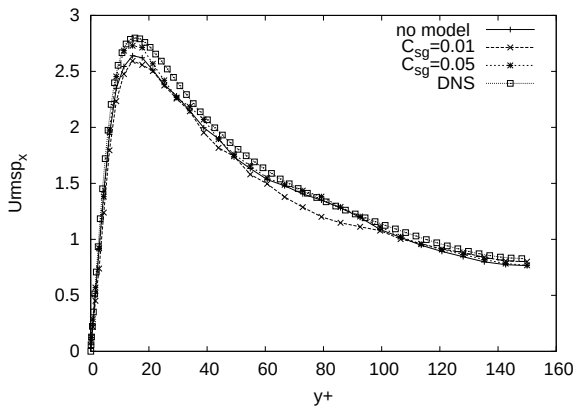

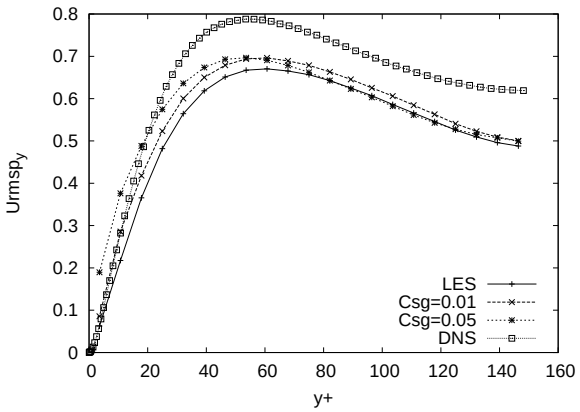

Figure 3. The r.m.s. of $St = 1$ particle velocity: a) streamwise, b) wall-normal. DNS (□), LES without model for particles (+), LES with SGS model with constant $C_{sg} = 0.01$ (×), LES with SGS model with constant $C_{sg} = 0.05$ (∗).

There is no significant difference between the temperature statistics of particles in LES with and without the model in the core of the flow, but near the walls ($y^+ < 10$) there is a change in the r.m.s. shape, depending on St. On the other hand, the effect of the subfilter particle dispersion model is not reflected in the probability density function (PDF) of particle temperature (Figs. 5 and 7); henceforth, we consider LES results without the SGS particle dispersion model.

The turbulent heat flux (Fig. 8) obtained from LES is in a qualitative agreement with the DNS data [4]. Also, a similar trend in both LES and DNS is observed, i.e., for increasing particle inertia the turbulent heat flux $\langle u\theta \rangle_p$ increases. The near-wall region is most affected by LES filtering and streamwise vortex rolls are not well resolved; therefore, the fluid velocity-temperature correlation coefficient $R_{u\theta} = \langle u\theta \rangle / u_{rms}\theta_{rms}$ is lower than in experiment (Fig. 9). For particles, the correlation increases with St, similarly as the turbulent heat flux.

The particle temperature PDF near the wall (Fig. 10) for $St = 1$ is in good agreement with the experimental data for fluid. Morover, a deviation from the normal distribution is observed. The "heavy tail" occurs in the region of lower temperatures, more pronounced, as the particle size increases. The effect may be due to the longer thermal relaxation time of heavy particles. They are more reluctant to transfer heat from the fluid in the near wall region, which results in

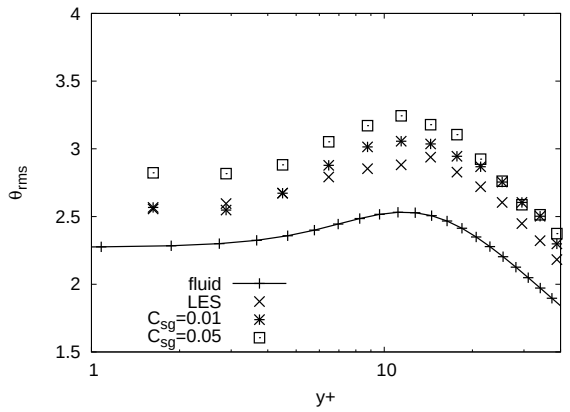

Figure 4. The r.m.s. particle temperature for St=1; DNS data [3]

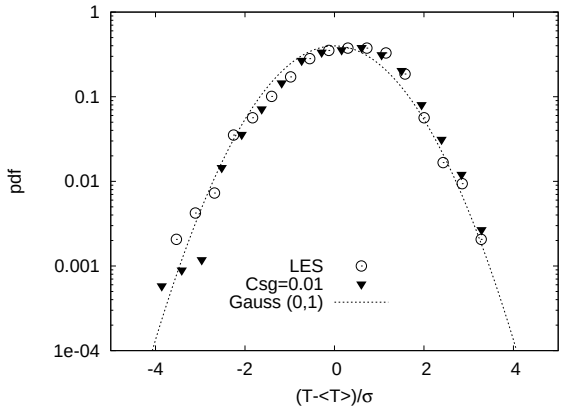

Figure 5. The PDF of particle temperature with and without the model at $y^+ = 3$; St=1

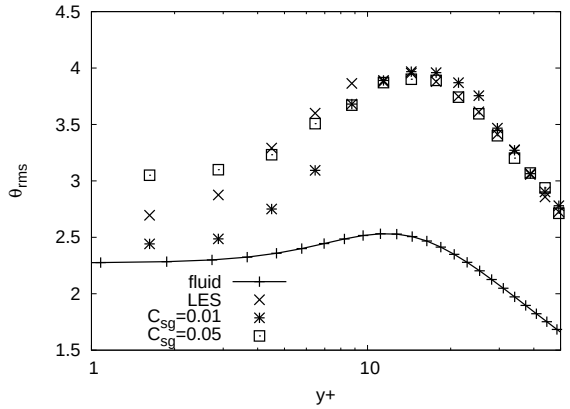

Figure 6. The r.m.s. particle temperature for $St = 25$; DNS data [3]

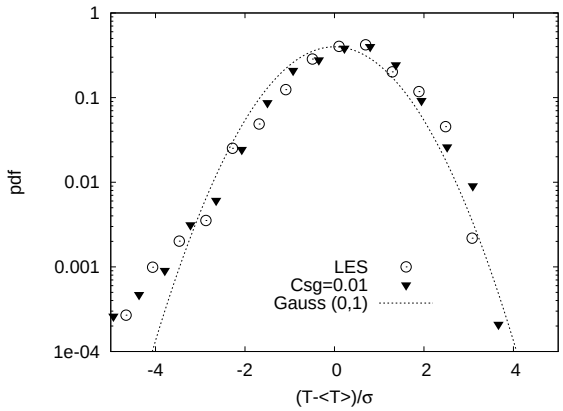

Figure 7. The PDF of particle temperature with and without the model at $y^+ = 3$; St=25

a greater number of cold particles. A similar situation is observed at the centre of the channel (Fig. 11), but now the "heavy tail" is on the hot particle side.

5. Concluding remarks

The LES simulation performed for turbulent heated channel flow with the dispersed phase is in a reasonable agreement with available DNS and experimental data. The results show some impact of the subfilter particle dispersion model. The presented model is of diffusion type, and although it recovers the kinetic energy of particles, it is known to alter the preferential concentration patterns. A solution to the problem may be in a structural model, enhancing near-wall structures of fluid velocity field. The r.m.s. particle temperature and the velocity-temperature correlation coefficients are found to be affected by the proposed model in the near-wall region. Moreover, the dispersed phase behaves similarily as in the DNS: with the increase of particle size comes a higher correlation of velocity and temperature. The PDF of particle temperature shows a non-gaussian behaviour, more pronounced for larger Stokes numbers.

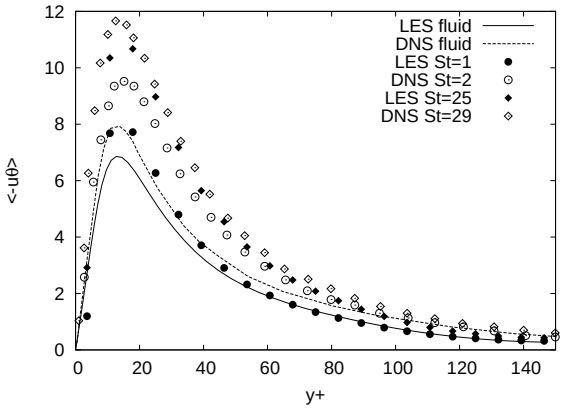

Figure 8. The turbulent heat flux; ref. DNS data [4]

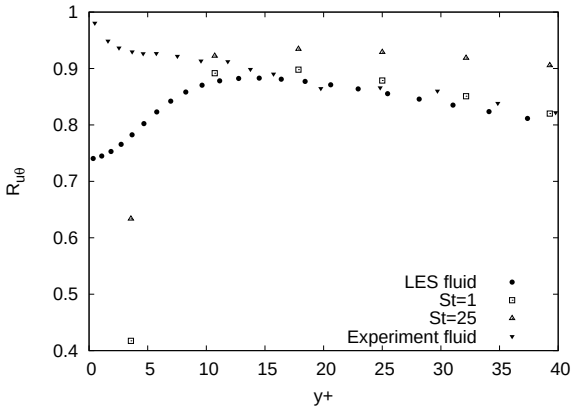

Figure 9. The correlation coefficient of temperature and streamwise velocity; experimental data [12]

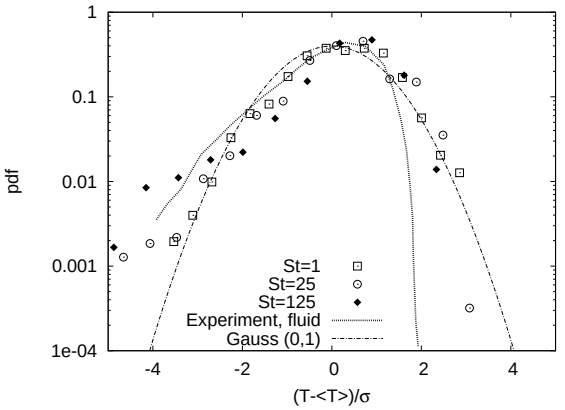

Figure 10. The particle temperature PDF at $y^+ = 3$; experimental data [12]

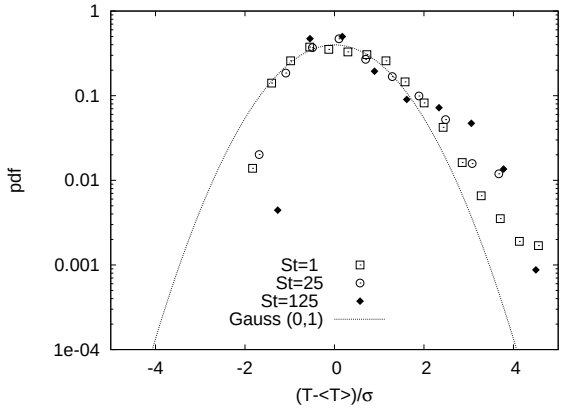

Figure 11. The particle temperature PDF at the centre of the channel

Acknowledgments

The work has been done in the framework of COST Action MP0806 "Particles in Turbulence". Calculations were carried out at the Academic Computer Center TASK in Gdańsk.

References

[1] Soldati A 2005 Appl. Math. & Mech. ZAMM **85** 683–699
[2] Marchioli C, Soldati A, Kuerten J, Arcen B, Tanière A, Goldensoph G, Squires K, Cargnelutti M and Portela L 2008 Int. J. Multiphase Flow **34** 879–893
[3] Kawamura H, Abe H and Matsuo Y 1999 Int. J. Heat Fluid Flow **20** 196–207
[4] Jaszczur M and Portela L 2008 Quality and Reliability of Large-Eddy Simulations ed Meyers J, Geurts B and Sagaut P (Springer) pp 343–354
[5] Pozorski J and Łuniewski M 2008 Quality and Reliability of Large-Eddy Simulations ed Meyers J, Geurts B and Sagaut P (Springer) pp 331–342
[6] Lilly D 1991 Phys. Fluids A **3** 1760
[7] Hagiwara Y 2011 Flow Turbulence Combust. **86** 343–367
[8] Pozorski J and Łuniewski M 2011 Quality and Reliability of Large-Eddy Simulations II ed Salvetti M, Geurts B, Meyers J and Sagaut P (Springer) pp 171–180
[9] Pozorski J and Apte S 2009 Int. J. Multiphase Flow **35** 118–128
[10] Yoshizawa Y 1986 Phys. Fluids **29** 2152–2164
[11] Kasagi N, Tomita Y and Kuroda A 1992 J. Heat Transfer **114** 598–606
[12] Antonia R, Krishnamoorthy V and Fulachier L 1988 Int. J. Heat Mass Transfer **31** 723–730